組織由来幹細胞への超音波遺伝子導入・培養・保存方法の検討

分担研究者　宮本義孝　名古屋大学医学系研究科　助教

研究要旨

　本研究では，母体外からの超音波照射により胎児標的組織（細胞）に目的遺伝子を導入し，遺伝子機能異常の出生前発現を低侵襲性に一定期間是正する安全性の高い胎児期遺伝子治療の確立を目的とする．胎児では，代謝・免疫・造血機能が一つの臓器（肝）に集約され，出生後の免疫学的トレランスを獲得しやすい．中でも，肝臓には肝実質細胞以外にも様々な細胞が共存し，そこには多分化能を有する幹細胞（肝幹細胞など）が数多く存在する．そこで，本年度は，プロジェクトの基盤技術である超音波遺伝子導入法を用い，移植・再生医療の新たな細胞源として注目され，比較的に入手しやすい脂肪由来幹細胞（Adipose tissue-derived stem cells: ASCs）に注目し，超音波照射による遺伝子導入実験を行った．まず，超音波造影剤として利用されているマイクロバブル（ソナゾイド）を用いて，マウス皮下脂肪組織から分離したASCsへの超音波遺伝子導入実験を行い，低い導入効率ではあるが，細胞内への遺伝子の取り込みが確認できた．また，ヒト由来幹細胞への利用を考え，その培養法と凍結保存の基礎検討も行った．

A．研究目的

　本研究では，母体外からの超音波照射により胎児標的組織（細胞）に目的遺伝子を導入し，遺伝子機能異常の出生前発現を低侵襲性に一定期間是正する安全性の高い胎児期遺伝子治療の確立を目的とする．胎児では，代謝・免疫・造血機能が一つの臓器（肝）に集約され，出生後の免疫学的トレランスを獲得しやすい．中でも，肝臓には肝実質細胞以外にも様々な細胞が共存し，そこには多分化能を有する幹細胞（肝幹細胞など）が数多く存在する．そこで，本年度は，プロジェクトの基盤技術である超音波遺伝子導入法を用い，移植・再生医療の新たな細胞源として注目され，比較的に入手しやすい脂肪由来幹細胞（Adipose tissue-derived stem cells: ASCs）を利用して，遺伝子導入実験を行った．また，これらの組織幹細胞は特定の遺伝子を導入することにより，移植する際の目的細胞へ分化誘導することが期待されている．現在，遺伝子導入研究は，遺伝子導入効率の点からウイルスベクターを用いたものが主流であるが，臨床応用と安全面を考慮すると，非ウイルスベクターを用いた超音波遺伝子導入法（ソノポレーション）も有力な手法の一つである．

　そこで，本研究では，ASCsへの超音波遺伝子導入の可能性について検証した．我々は，まず，マウス皮下脂肪組織を採取し，分離して得られたASCsを本実験に用いた．また，ヒト由来幹細胞への利用を考え，その培養法と凍結保存について検証したので，あわせて報告する．以下に、本年度の課題項目を示す．

1）ASCsへの超音波遺伝子導入法の検証．

2）ヒト可溶化羊膜(HSAP)を用いたASCsの培養と機能評価．

3）ヒトASCsの凍結保存と機能評価．

B．研究方法

B-1 ASCsへの超音波遺伝子導入法の検証

【細胞】マウス皮下脂肪組織（C57BL/6, 雌, 10週齢）を採取し，コラゲナーゼを用いて脂肪細胞を分離しSVFを得た．SVFを37℃, 5%CO_2下で培養し，最終的に，骨・脂肪に分化可能なASCsを得た．以下に，その培養液の組成を示す（DMEM/F12 (Invitrogen), 20%FBS (Bench Mark), 1%Penicillin Sereptomycin (Invitrogen)）．

【材料】哺乳類細胞レポーターベクター として，Lac Z遺伝子を含むプラスミドDNA（pCMVβVector (PT2004-5); Clontech）を用いた．超音波造影剤として，臨床検査で使用されているソナゾイド（第一三共株式会社）を用いた．

【方法】96穴培養皿（Nunc）上に，ASCsを播種し（2x10^4 cells/100uL），37℃, 5%CO_2下で24時間培養した．細胞培養後，培養皿内の各ウェルに対して，超音波照射条件を設定し，細胞へのダメージを評価した（周波数: 3.122MHz, 印加電圧30-60V, Duty比50%, Burst Rate 2.0Hz, Duration 10sec, 出力強度0.61-2.20 W/Cm^2）．超音波遺伝子導入装置はソノポール4000（KTAC-4000, NEPAGENE），超音波プローブはドーム前方照射型8mmTを用いた．細胞生存率の評価方法として，高感度水溶性ホルマザンを生成する新規テトラゾリウム塩 WST-8 を発色基質として用いた評価方法（Cell Counting Kit-8; DOJINDO）

を利用した.

遺伝子導入実験は,プラスミド DNA とマイクロバブルを混和したのち,直ちに,96 ウェル内の ASCs の培地を交換し,超音波を照射して,マイクロバブルを破砕した.マイクロバブル破砕後,培地交換を繰り返し,ソナゾイドの被膜(ホスファチジルセリンナトリウム)を除去した.除去後,ウェル内に細胞培養液を加え,37°C,5%CO$_2$ 下で 24 時間培養した.細胞内への遺伝子導入の評価方法として,細胞中の β-ガラクトシダーゼ活性を検出し,Lac Z 遺伝子が発現する細胞を同定した(X-Gal Staining Assay Kit (A10300K); Genlantis).

B-2 ヒト可溶化羊膜(HSAP)を用いた ASCs の培養と機能評価

【細胞】上記の手法と同じ(B-1)
【材料】培養皿コート剤として,桜川らが開発したヒト可溶化羊膜(HSAP)を利用した.
【方法】12 穴培養皿(プラスチック培養皿,コラーゲンコート培養皿,HSAP コート培養皿)上に,ASCs を 1 x 10^5 cells /ml 播種し,37°C,5%CO$_2$ 下で培養した.所定期間培養後,各培養皿における細胞の生死と増殖率(LIVE/DEAD Assay, WST-1 Assay)および細胞の形態を観察した.また,脂肪および骨への分化の確認方法として,Oil Red O 染色および Von Kossa 染色を用いた.

B-3 ヒト ASCs の凍結保存と機能評価

【細胞】ヒト ASCs は,インフォームドコンセントにより供給された Zen-Bio 社製,継代数 2 を使用した(# ASC-F, LotASC062801; sex/age/BMI (average)/Number of patients: Female/37/23.29/1 (single)).
【材料】ヒト ASCs の培養において,Zen-Bio 社製の維持用培地(# PM-1),脂肪分化誘導培地(# DM-2)および骨分化誘導培地(# OB-1)を用いた.また,セーレン株式会社より,カイコの繭由来タンパク質セリシン(平均分子量約 3 万)を提供して頂き,本研究に用いた.
【方法】25cm^2 培養フラスコ(NUNC)上に,ヒト ASCs を 2×10^5 細胞/5mL 播種し,37 °C,5%CO$_2$ インキュベータ内で継代培養を行った(継代数 5, and 7).細胞用培養液は,PM-1 を用いた.ヒト ASCs を継代培養したのち,各凍結保存液を用いて,細胞密度 5×10^6 cells/ml で凍結保存した.凍結保存液として,基本凍結保存液(PM-1 培地+10%DMSO),セルバンカー2(日本全薬工業),セリシン含有凍結保存液(PM-1 培地(serum-free)+10%DMSO, 1%セリシン, 0.1mol/L マルトース)の 3 種類を使用した.凍結方法は,調製済みの各サンプルチューブを,バイセル凍結処理容器(日本フリーザー(株))に入れ,−80°C ディープ

フリーザーで静置し,1-3 ヶ月間保管した.融解は,37°C 恒温槽中で急速解凍した.融解後,ヒト ASCs の生細胞率をトリパンブルー排除能(最終濃度 0.2%)で測定した.また,細胞の増殖率は,Cell Counting Kit-8(CCK-8; DOJINDO)を用いた.また,ヒト ASCs から脂肪および骨への分化の確認方法として,Oil Red O 染色および Von Kossa 染色を用いた.

(倫理面への配慮)
名古屋大学
実験動物に関して,「動物の愛護及び管理に関する法律」(昭和 48 年法律第 105 号),「実験動物の飼養及び管理等に関する基準」(昭和 55 年総理府告示第 6 号)及び「名古屋大学動物実験指針」に基づき,適正な使用及び取り扱いを行う.
国立成育医療センター
ヒト肝組織・細胞を使用するための倫理審査:国立成育医療センター・倫理委員会審査より(H16. 8. 10)受付番号 98,「ヒト肝の創薬研究資源化」,安全対策:遺伝子組換え生物等の使用等の規制による生物の多様性の確保に関する法律(カルタヘナ法)において,バイオセーフティーレベル 2 の設備は設置済み

C. 研究結果
C-1 ASCs への超音波遺伝子導入法の検証
超音波照射条件を設定し,マイクロバブル(0-40% v/v 細胞培養液)の量を変えながら,ASCs へのダメージを検証した.その結果,マイクロバブルの量が 5-10%の時に効率よく破砕された.得られた知見をもとに,超音波照射条件(周波数: 3.122MHz, Duty 比 50%, Burst Rate 2.0Hz, Duration 10sec, 出力強度 1.15-1.21 W/Cm2)を設定し,マイクロバブル(10% v/v 培養培地溶液),プラスミド DNA(20ug/mL)を加え実験を行ったところ,低い導入効率ではあるが,ASCs への遺伝子発現が確認できた.

C-2 ヒト可溶化羊膜(HSAP)を用いた ASCs の培養と機能評価
ASCs の培養において,プラスチック培養皿と比べて,HSAP コート培養皿は,細胞増殖亢進作用を示し,細胞の形態も良好であった.また,分化誘導を行った ASCs は,脂肪および骨への形態変化が見られた.

C-3 ヒト ASCs の凍結保存と機能評価
ヒト ASCs の生存率を比較すると,3 種類の保存液(基本凍結保存液,セルバンカー2,セリシン含有凍結保存液)の間で有意差は見られなかった(>95%).また,ヒト ASCs の増殖能,多分化能(脂肪や骨)を比較すると,セリシン含有凍結保存液,セルバンカ

ー2を用いた保存液が，基本凍結保存液と比べて，有意であることが確認できた．

D. 考察
　本研究において，標的である肝臓には肝実質細胞以外にも様々な細胞が共存し，そこには多分化能を有する幹細胞（肝幹細胞など）が数多く存在する．前年度は肝細胞を中心に検討したが，本年度はそれ以外の幹細胞に着目し検討した．中でも，移植・再生医療の新たな細胞源として注目されており，入手しやすい脂肪由来幹細胞(Adipose tissue-derived stem cells: ASCs) を幹細胞モデルとして用いて，超音波遺伝子導入実験を行った．その結果，ASCs での遺伝子発現効率は非常に低かったが，今後，超音波照射条件を最適化することにより，導入効率の改善が期待できる．特に，現在使用中の市販の超音波照射装置では，照射条件等に限界があるため，分担研究者と連携して，装置開発を含めた検証を進めてゆく．また，本年度は，ASCs の培養法と凍結保存の基礎検証についても行った．可溶化羊膜(HSAP)およびカイコの繭由来タンパク質セリシンを利用することにより，細胞培養に有効かつ安定に保存・供給できる可能性が示された．

E. 結論
　本研究では，組織由来幹細胞の一つである ASCs に対して，マイクロバブルと超音波照射による遺伝子導入実験の検討を行い，低い導入効率ではあるが，細胞内への遺伝子の取り込みが確認できた．今後，対象となる肝臓に存在する幹細胞（肝幹細胞など）での検証を行う．

F. 健康危険情報
　統括研究報告書に記載

G. 研究発表
1.論文発表
1. Miyamoto Y, Oishi K, Yukawa H, Noguchi H, Sasaki M, Iwata H, Hayashi S. Cryopreservation of human adipose tissue-derived stem/progenitor cells using the silk protein sericin. Cell Transplant accept
2. Miyamoto Y, Teramoto N, Hayashi S, Enosawa S. An improvement in the attaching capability of cryopreserved human hepatocytes by a proteinaceous high molecule, Sericin, in the serum-free solution. Cell Transplant in press
3. 宮本義孝, 大石幸一, 湯川博, 野口洋文, 佐々木真宏, 岩田久, 林衆治. ヒト脂肪組織由来幹細胞における細胞凍結保存液の検討. 低温生物工学会誌. 56(1):55-58; 2010

2.学会発表
1. Miyamoto Y, Enosawa S. Cryopreservation of primary

hepatocytes using oligosaccharides. 238th ACS National Meeting & Exposition, Washington, DC, USA, 8/16-20 2009.
2. Miyamoto Y, Oishi K, Yukawa H, Noguchi H, Sasaki M, Iwata H, Hayashi S. Refreezing on Human Adipose Tissue-Derived Stem/Progenitor Cell by Supplementation of Silk Protein Sericin in the Freezing Medium. 238th ACS National Meeting & Exposition, Washington, DC, USA, 8/16-20 2009.
3. Miyamoto Y, Oishi K, Yukawa H, Noguchi H, Sasaki M, Iwata H, Hayashi S. Cryopreservation of human adipose tissue-derived stem/progenitor cells using the silk protein sericin. Cryo2009 46th Annual Meeting of the Society for Cryobiology. Sapporo, Japan, 7/19-23, 2009.
4. 宮本義孝, 腰高由美恵, 湯川博, 野口洋文, 岩田久, 小林護, 加茂功, 桜川宣男, 林衆治. ヒト可溶化羊膜(HSAP)の脂肪組織由来幹細胞への影響. 第 9 回日本再生医療学会総会, 広島, 2010 年 3 月 18-19 日.
5. 宮本義孝, 金季利, 上野瞳, 林衆治, 千葉敏雄. 脂肪組織由来幹細胞を用いた超音波遺伝子導入法の検討. 第 32 回日本分子生物学会年会. 横浜, 2009 年 12 月 9-12 日.
6. 宮本義孝, 腰高由美恵, 湯川博, 野口洋文, 岩田久, 小林護, 加茂功, 桜川宣男, 林衆治. ヒト可溶化羊膜(HSAP)を用いた脂肪組織由来幹細胞の培養と機能評価. 第 32 回日本分子生物学会年会. 横浜, 2009 年 12 月 9-12 日.

H. 知的財産権の出願・登録状況
1. 特許取得
　なし
2. 実用新案登録
　なし
3. その他
　なし

別紙5

研究成果の刊行に関する一覧表

書籍

著者氏名	論文タイトル名	書籍全体の編集者名	書籍名	出版社名	出版地	出版年	ページ
本年度は該当なし							

雑誌

発表者氏名	論文タイトル名	発表誌名	巻号	ページ	出版年
元文姫，上野瞳，穂刈玲，柿本隆志，久野周一，土屋玲子，宮本義孝，絵野沢伸，**千葉敏雄**	マイクロバブルと超音波によるin vivo遺伝子導入の試み	第32回日本分子生物学会年会	2009	261	2009
穂苅玲，上野瞳，元文姫，久野周一，柿本隆志，土屋玲子，宮本義孝，絵野沢伸，**千葉敏雄**	エコーガンによる非ウイルスベクターの細胞内への導入	第32回日本分子生物学会年会	2009	259	2009
土屋玲子，上野瞳，元文姫，穂苅玲，久野周一，柿本隆志，宮本義孝，絵野沢伸，葭仲潔，松本洋一郎，**千葉敏雄**	超音波とマイクロバブルによる胎児遺伝子治療の検討	第8回日本超音波治療研究会	2009	22	2009
Yamada M, Hamatani T, Akutsu H, Chikazawa N, Kuji N, Yoshimura Y, **Umezawa A.**	Involvement of a novel preimplantation-specific gene encoding the high mobility group box protein Hmgpi in early embryonic development	Hum Mol Genet	19(3)	480-493	2010

Takahashi H, Toyoda M, Birumachi J, Horie A, Uyama T, Miyado K, Matsumoto K, Saito H, **Umezawa A**	Shortening of human cell life span by induction of p16ink4a through the platelet-derived growth factor receptor beta	J Cell Physiol	221(2)	335-342	2009
Akutsu H, Miura T, Machida M, Birumachi JI, Hamada A, Yamada M, Sullivan S, Miyado K, **Umezawa A**	Maintenance of pluripotency and self-renewal ability of mouse embryonic stem cells in the absence of tetraspanin CD9	Differentiation	78(2-3)	137-142	2009
Yazawa, T, Inanoka Y, Mizutani T, Kuribayashi M, **Umezawa A**, Miyamoto K	Liver receptor homolog-1 regulates the transcription of steroidogenic enzymes and induces the differentiation of mesenchymal stem cells into steroidogenic cells	Endocrinology	150(8)	3885-3893	2009
岡本旭生, 橘理恵, 葭仲潔, 高木周, **松本洋一郎**	マイクロバブルを援用した超音波遺伝子導入	第8回日本超音波治療研究会	2009	18	2009
Kohji Masuda, Yusuke Muramatsu, Sawami Ueda, Ryusuke Nakamoto, Yusuke Nakayashiki, and Ken Ishihara	Active Path Selection of Fluid Microcapsules in Artificial Blood Vessel by Acoustic Radiation Force	Japanese Journal of Applied Physics	48(7)	07GK03	2009
Ryusuke Nakamoto, Hayato Yamauchi, Yusuke Muramatsu, **Kohji Masuda**, Yoshitaka Miyamoto and Toshio Chiba	Evaluation of trapping performance of fluid microcapsules to the parameter variation in acoustic radiation	Proc. of the 30th Symposium on Ultrasonic Electronics, Nov. 2009, Kyoto	2009	545-546	2009

Kohji Masuda, Nobuyuki Watarai, Ren Koda, Ryusuke Nakamoto and Yusuke Muramatsu	Production of local acoustic radiation force to constrain microcapsules from diffusion in blood vessel	Proc. of the 30th Symposium on Ultrasonic Electronics, Nov. 2009, Kyoto	2009	529-530	2009
Kohji Masuda, Ryusuke Nakamoto, Yusuke Muramatsu, Yoshitaka Miyamoto, Keri Kim, and Toshio Chiba	Study to trap fluid microcapsules in artificial blood vessel by producing local acoustic radiation force	IFMBE Proceedings (World Congresson Medical Physics and Biomedical Engineering)	Vol.25	206-207	2009
Kohji Masuda, Ryusuke Nakamoto, Yusuke Muramatsu, Yoshitaka Miyamoto, Keri Kim and Toshio Chiba	Active Control of Microcapsules in Artificial Blood Vessel by producing Local Acoustic Radiation Force	Proc. of 31st Annual International Conference of the IEEE EMBS	2009	295-298	2009
中元隆介, 村松悠佑, 上田沢美, 中屋敷悠介, **桝田晃司**, 宮本義孝, 千葉敏雄	局所的音響放射力による流体中のマイクロカプセルの安定な捕捉法の検討	第48回日本生体医工学会大会プログラム	2009	CD-ROM	2009
宮本義孝, 金季利, 上野瞳, 林衆治, 千葉敏雄	脂肪組織由来幹細胞を用いた超音波遺伝子導入法の検討	第32回日本分子生物学会年会	2009	264	2009
宮本義孝, 腰高由美恵, 湯川博, 野口洋文, 岩田久, 小林護, 加茂功, 桜川宣男, 林衆治	ヒト可溶化羊膜(HSAP)の脂肪組織由来幹細胞への影響	日本再生医療学会雑誌	9 Suppl.	291	2010
宮本義孝, 大石幸一, 湯川博, 野口洋文, 佐々木真宏, 岩田久, 林衆治.	ヒト脂肪組織由来幹細胞における細胞凍結保存液の検討	低温生物工学会誌	56(1)	55-58	2010

3P-0872　ポスター2009-12-11　第 17 会場マイクロバブルと超音波による in vivo 遺伝子導入の試み Gene transduction using ultrasound with non-virus vector in vivo

○元 文姫 1, 上野 瞳 1, 穂苅 玲 1, 柿本 隆志 1, 久野 周一 1, 土屋 玲子 1, 宮本 義孝 2, 絵野沢 伸 1, 千葉 敏雄 1

○Wenji Yuan1, Hitomi Ueno1, Rei Hokari1, Takashi Kakimoto1, Shuichi Kuno1, Reiko Tsuchiya1, Yoshitaka Miyamoto2, Shin Enosawa1, Toshio Chiba1(1 成育・臨床研究開発部,2 名古屋大・医) (1Department of Clinical Research & Development, NCCHD,2Department of Advanced Medicine inBiotechnology and Robotics, Nagoya Univ. Grad. Sch. of Med.)

【目的】ウイルスベクターを用いた遺伝子治療は臨床応用されているが、その治療効果や安全性についてはまだ多くの課題が残されている。一方、非ウイルスベクターは、ウィルスベクターに比べ安全性には問題ないものが多いが、現在までの技術では in vivo での発現効率が充分ではなく、臨床応用は難しいとされてきた。本研究では、非ウイルスベクターと超音波照射装置を用いて、従来の出生後治療に先行する出生前遺伝子治療、すなわち安全かつ効率的な低侵襲遺伝子治療システムを開発することを目的としている。今回我々の用いた超音波遺伝子導入法は、超音波とマイクロバブルを併用して、一時的に細胞膜に微細穴を開けて遺伝子を導入させる技術である。この技術を用いて、マウス肝への遺伝子導入の条件を検討した。【方法】ペントバルビタール麻酔下で、5 週齢 ICR 系雌性マウス（２０ｇ〜２８ｇ）を開腹後、肝左葉表面直下へ GFP プラスミド（３０μg）とマイクロバブル (Sonazoid,第一三共）の混合液（２０μL）を注射後、超音波を照射し、腹部を縫合した。超音波照射装置は Sonitron 2000V（Nepagene）を用いた。一定時間後にマウスを屠殺して肝を摘出、投与葉（左葉）と非投与葉における遺伝子発現レベルを観察した。【結果・考察】超音波照射２４時間後に GFP 遺伝子発現が観察された。発現は４８時間後にさらに５倍程度に増強した。マイクロバブルの割合、超音波の強度、照射時間、周波数が異なると発現細胞の分布（注入部位からの距離、深さ）や割合が変わることが確認できた。これらの中で遺伝子導入効率を高めるパラメーターは、照射時間と周波数で、それぞれ１分間、１MHz の時が最高であった。しかしながら、同条件では超音波プローブが接する肝表面に火傷様の損傷が生じた。GFP 発現は創傷部あるいはその近傍よりもむしろやや深部に見られた。創傷は周波数よりむしろ照射時間が影響すると考えられ、3MHz の 20 秒間照射は前記条件より軽度であり、一方、GFP 発現はやや低下したに留まった。

2P-0880　ポスター2009-12-10　第 17 会場エコーガンと非ウイルスベクターによる細胞内への遺伝子導入 Gene transduction using ultrasound with non-virus vector in vitro

○穂苅 玲 1, 上野 瞳 1, 元 文姫 1, 久野 周一 1, 柿本 隆志 1, 土屋 玲子 1, 宮本 義孝 2, 絵野沢 伸 1, 千葉 敏雄 1○Rei Hokari1, Hitomi Ueno1, Wenji Yuan1, Shuichi Kuno1,Takashi Kakimoto1, Reiko Tsuchiya1, YoshitakaMiyamoto2, Shin Enosawa1,Toshio Chiba1(1 成育・臨床研究開発,2 名古屋大・医） (1Department of Clinical Research & Development, NCCHD,2Department of Advanced Medicine in Biotechnology and Robotics, Nagoya Univ. Grad. Sch. of Med.)

　我々は、ムコ多糖症など先天代謝異常症における欠失機能を胎児期の遺伝子導入により是正し、出生後治療の効率的支援を目指している。本研究では、非ウイルスベクター（プラスミド DNA）とマイクロバブルを用い、超音波装置（Nepagene 社 SonoPore-KTAC4000,Sonitron2000V）によるマイクロバブル破砕時に生じるキャビテーション（微細気泡）を利用して標的細胞への遺伝子導入を試みた。

【方法】マイクロバブルはペルフルブタンガス封入造影剤のソナゾイド（第一三共）を使用した。肝芽腫由来 HepG2 細胞及び牛大動脈内皮細胞由来 HH 細胞、マウス線維芽細胞 NIH3T3 細胞を用いて GFP プラスミド DNA（pTracerA（invitrogen）、ｐEGFP(Clontech)）の導入効率を、超音波の照射条件を変えて検討した。また、キャビテーションによる細胞傷害の検討を行った。【結果と考察】導入効率に対し、マイクロバブルの濃度（5〜20%）、照射時間（15 秒〜2 分）は特に影響を及ぼさなかった、しかしながら、照射強度は、1.0W/cm² 以上で発現率の向上が確認できた。また、pTracerA プラスミドよりも pEGFP プラスミドを試用した時に効率よく発現が得られた。超音波照射を行うと、照射域の細胞が剥離した。この部分の細胞を再播種したところ、生着し、大半の細胞で EGFP の発現が認められた。胎児治療では、胎児のみならず、母体への侵襲もできる限り低く抑えたい。その点、超音波を利用した本遺伝子導入法は適すると考えられる。今後、細胞障害がより軽度かつ導入効率の高い条件を、機器の改良も含め検討したい。

１３超音波とマイクロバブルによる胎児遺伝子治療の検討

土屋玲子、上野瞳、元文姫、穂苅玲、久野周一、柿本隆志、宮本義孝、絵野沢伸、葭仲潔、松本洋一郎、千葉敏雄国立成育医療センター臨床研究開発部

【目的】超音波遺伝子導入法（ Sonoporation）は超音波によって細胞膜に一時的に微細な穴を開けることで遺伝子を導入させる技術であり、マイクロバブルを目的遺伝子と共に併用する事で遺伝子導入効率が向上することが知られている。我々はこの方法により、超音波と非ウィルスベクターを用いた安全かつ低侵襲な遺伝子治療方法を開発し、胎児や新生児への治療成績と予後を改善するシステムの確立を目的としている。【方法】麻酔下において開腹した妊娠マウスの子宮を露出し、子宮内のマウス胎仔の組織へ造影剤マイクロバブル Sonazoid と GFP プラスミド DNA の混合溶液を注入した。注入後直ちに子宮外からの超音波照射を行って母体腹部を縫合し、照射後 24~48 時間後に胎仔臓器を回収して GFP の発現を確認した。【結果・考察】マイクロバブルとの併用で遺伝子導入効率の向上が確認され、超音波を用いたこの遺伝子導入法は、今後の新たな胎児遺伝子治療に応用可能であることが示唆された。

Involvement of a novel preimplantation-specific gene encoding the high mobility group box protein *Hmgpi* in early embryonic development

Mitsutoshi Yamada[1,2], Toshio Hamatani[1,*], Hidenori Akutsu[2], Nana Chikazawa[1,2], Naoaki Kuji[1], Yasunori Yoshimura[1] and Akihiro Umezawa[2]

[1]Department of Obstetrics and Gynecology, Keio University School of Medicine, 35 Shinanomachi Shinjyuku-ku, Tokyo 160-8582, Japan and [2]Department of Reproductive Biology, National Research Institute for Child Health and Development, 2-10-1 Ohkura Setagaya-ku, Tokyo 157-8535, Japan

Mining gene-expression-profiling data identified a novel gene that is specifically expressed in preimplantation embryos. *Hmgpi*, a putative chromosomal protein with two high-mobility-group boxes, is zygotically transcribed during zygotic genome activation, but is not transcribed postimplantation. The *Hmgpi*-encoded protein (HMGPI), first detected at the 4-cell stage, remains highly expressed in pre-implantation embryos. Interestingly, HMGPI is expressed in both the inner cell mass (ICM) and the trophectoderm, and translocated from cytoplasm to nuclei at the blastocyst stage, indicating differential spatial requirements before and after the blastocyst stage. siRNA (siHmgpi)-induced reduction of *Hmgpi* transcript levels caused developmental loss of preimplantation embryos and implantation failures. Furthermore, reduction of *Hmgpi* prevented blastocyst outgrowth leading to generation of embryonic stem cells. The siHmgpi-injected embryos also lost ICM and trophectoderm integrity, demarcated by reduced expressions of Oct4, Nanog and Cdx2. The findings implicated an important role for *Hmgpi* at the earliest stages of mammalian embryonic development.

INTRODUCTION

Preimplantation development encompasses the period from fertilization to implantation. Oocytes cease developing at metaphase of the second meiotic division, when transcription stops and translation is reduced. After fertilization, sperm chromatin is reprogrammed into a functional pronucleus and zygotic genome activation (ZGA) begins, whereby the maternal genetic program governed by maternally stored RNAs and proteins must be switched to the embryonic genetic program governed by *de novo* transcription (1,2). Our previous gene expression profiling during preimplantation development revealed distinctive patterns of maternal RNA degradation and embryonic gene activation, including two major transient 'waves of *de novo* transcription' (3). The first wave during the 1- to 2-cell stage corresponds to ZGA. The second wave during the 4- to 8-cell stage, known as

mid-preimplantation gene activation (MGA), induces dramatic morphological changes to the zygote including compaction and blastocele formation, particularly given that few genes show large expression changes after the 8-cell stage. ZGA and MGA together generate a novel gene expression profile that delineates the totipotent state of each blastomere at the cleavage stage of embryogenesis, and these steps are prerequisite for future cell lineage commitments and differentiation. The first such differentiation gives rise to the inner cell mass (ICM), from which embryonic stem (ES) cells are derived, as well as the trophectoderm at the blastocyst stage. However, the molecular regulatory mechanisms underlying this preimplantation development and ES-cell generation from the ICM remain unclear.

Induced pluripotent stem (iPS) cells are ES cell-like pluripotent cells, generated by the forced expression of defined factors in somatic cells, including Pou5f1/Oct4, Sox2, Klf4

---

*To whom correspondence should be addressed. Tel: +81 353633819; Fax: +81 332261667; Email: t-hama@sc.itc.keio.ac.jp

and Myc (4). These iPS factors are thought to reprogram somatic nuclei in a somewhat similar way as ooplasm does in reconstructed oocytes by nuclear transfer (NT). However, with the exception of Oct4, these factors are not highly expressed maternally in oocytes, and only increased by zygotic transcription during preimplantation, based on expression sequence tag (EST) frequencies in Unigene cDNA libraries and microarray data from oogenesis to preimplantation development (5). Although pluripotency is achieved within 2 days in NT embryos reconstructed with a somatic nucleus, it takes approximately 2 weeks for the establishment of iPS cells. Such immediate induction of pluripotency during preimplantation development is attributed to well-organized transcriptional regulation, i.e. waves of transcription whereby maternal gene products trigger ZGA, which in turn fuels MGA. On the other hand, the forced simultaneous transcription of iPS factors in somatic cells does not efficiently induce these waves of transcription, and it takes a long time to activate the other genes necessary for pluripotency. Studying transcriptional regulation during preimplantation development would therefore also help unravel the establishment of iPS cells as well as pluripotency in these cells.

Large-scale EST projects (6–8) and DNA microarray studies (3,9–11) have revealed many novel genes zygotically expressed during preimplantation development. Very few of these genes, however, are exclusively expressed in preimplantation embryos (12), and such genes ought to have important roles during preimplantation development. For example, Zscan4, a novel transcription factor, is expressed specifically in 2-cell stage embryos and a subset of ES cells (13). Reduction of Zscan4 transcript levels by siRNAs delays progression from the 2-cell to the 4-cell stage, and produces blastocysts that neither implant *in vivo* nor proliferate in blastocyst outgrowth culture. Thus, a transcription factor expressed exclusively in preimplantation embryos is potentially a key regulator of global gene expression changes during preimplantation development. On the other hand, reprogramming gene expression during ZGA and MGA requires considerable changes in chromatin structure (14–16), and modulation of chromatin folding affects access of regulatory factors to their cognate DNA-binding sites. This modulation can be achieved by loosening the chromatin structure, by disrupting the nucleosome structure, by DNA bending and unwinding, and by affecting the strength of DNA-histone interactions via postsynthetic modifications of histones (17,18). Many of these structural changes are mediated by a large and diverse superfamily of high-mobility-group (HMG) proteins, which are the second most abundant chromosomal proteins after histones (18).

This study identified a novel preimplantation-specific gene, *Hmgpi*, which encodes a chromosomal protein containing HMG box domains. It reports a detailed expression analysis of *Hmgpi* and the *Hmgpi*-encoded protein (HMGPI), which was translocated from the cytoplasm to nuclei at the blastocyst stage. Loss-of-function studies were also conducted using siRNA technology. The siRNA-induced reduction in *Hmgpi* expression caused developmental loss at preimplantation stages and hampered implantation through reduced proliferation of both ICM-derived cells and trophectodermal cells during peri-implantation development.

RESULTS

Gene structure of a preimplantation-stage-specific gene, *Hmgpi*

In silico analysis identified *Hmgpi* (an **HMG**-box protein, preimplantation-embryo-specific) as a preimplantation-stage-specific gene encoding a chromosomal protein containing HMG box domains. The *Hmgpi* transcript levels are probably upregulated during ZGA (1- to 2-cell stages) to peak at the 4-cell stage, based on gene expression profiling (3,9) (Fig. 1A). Using the public expressed-sequence tag (EST) database, 16 cDNA clones were found exclusively in preimplantation-embryo libraries (2- to 8-cell stages) (Fig. 1B). One of these contained the full *Hmgpi* gene coding sequence (AK163257) (Fig. 1C), spanning 2579 bp and split into two exons, which encode a protein of 394 amino acids (aa) (NP_001028965) harboring a SANT domain ('SWI3, ADA2, N-CoR, and TFIIIB' DNA-binding domain) and two HMG-box domains, based on SMART domain prediction analysis (19) (Fig. 1C). In the NCBI Gene database, the *Hmgpi* gene is called Ubtf-like 1 (*Ubtfl1*) based on aa sequence similarity (36% identity and 58% positives by BLAST) to *Ubtf*-encoded protein 'upstream binding transcription factor', which contains a SANT domain and six HMG-box domains. Two rat homologs (*Ubtfl1* and *RGD1304745*) and three human homologs (*UBTFL1-3*) of the mouse *Hmgpi* were identified by BLASTing of NP_001028965 against the NCBI nucleotide database. Pairwise alignment scores by BLAST of amino acid sequences for rat and human homologs are 72.3–72.5% and 53.8–54.1%, respectively (Fig. 1D and Supplementary Material, Table S1), while those for nucleotide sequences are 83.7 and 66.8–67.0%, respectively. All these human homologs were predicted by *in silico* genome-based analysis, and have no ESTs in the Unigene database. The absence of human ESTs may reflect the paucity of cDNA libraries of human preimplantation embryos in the Unigene database, despite specific expression of the Hmgpi gene in human preimplantation embryos. Based on the number and the type of HMG-box domains, this novel protein could also be categorized into the HMG-box family (HMGB). A dendrogram of aa sequence similarity in HMG family proteins indicates two HMG subgroups (Fig. 1E). One includes the HMG-nucleosome binding family (HMGN) and the HMG-AT-hook family (HMGA), and the other is HMGB that includes HMGPI. All members of HMGB contain two HMG-box domains ('HMG-box' or 'HMG-UBF_HMG-box').

Expression of the *Hmgpi* gene and protein

First, we experimentally confirmed the preimplantaion-stage-specific expression pattern of *Hmgpi* suggested by the *in silico* analysis. Northern blot analysis using a mouse multiple tissue poly(A)RNA panel (FirstChoice® Mouse Blot 1 from Ambion, Austin, TX, USA) failed to detect expression of the *Hmgpi* gene (data not shown). While RT–PCR analysis using cDNA isolated from mouse adult tissues and fetuses (E7, E11, E15 and E17) also failed to show *Hmgpi* expression, RT–PCR analysis for preimplantation embryos indicated *Hmgpi* expression from the 2-cell embryo to the blastocyst
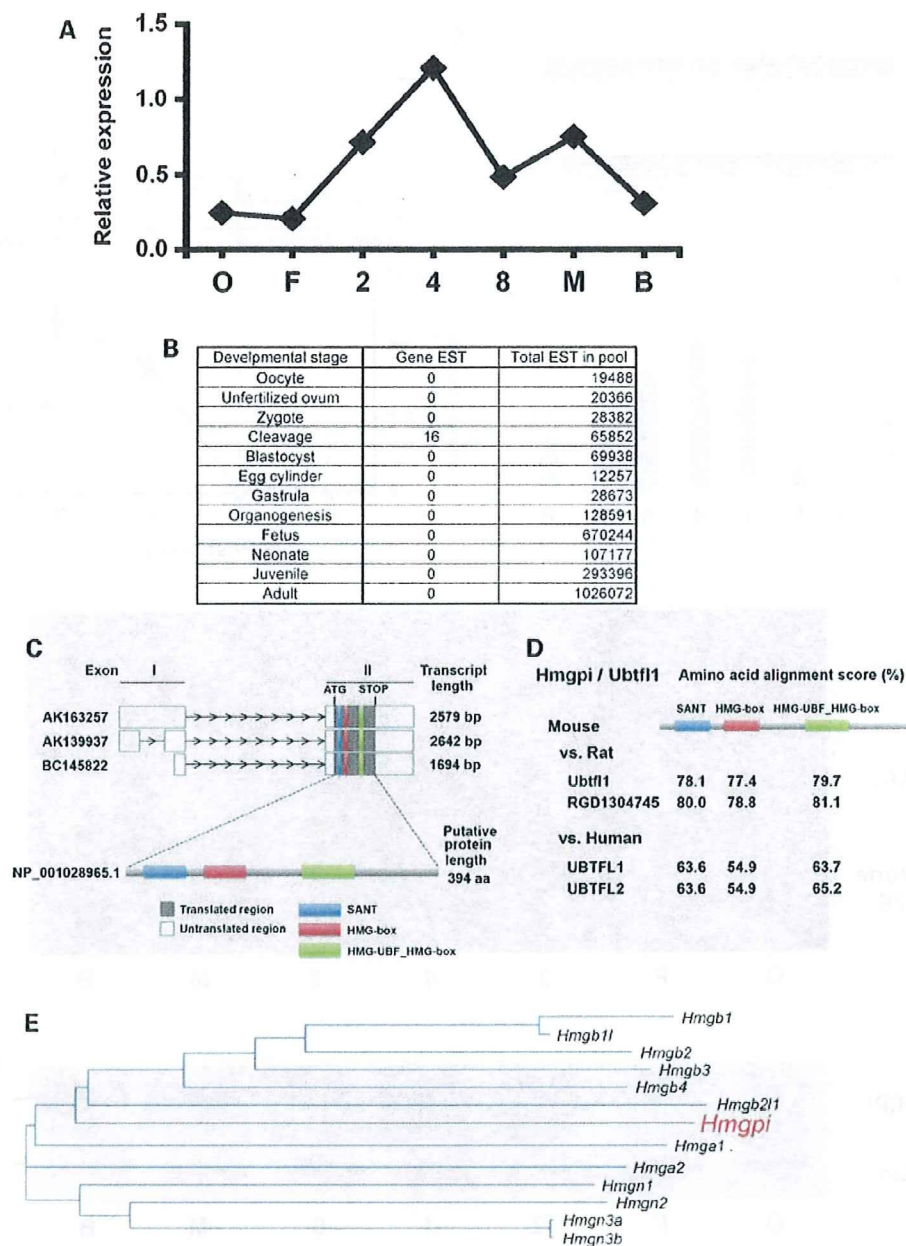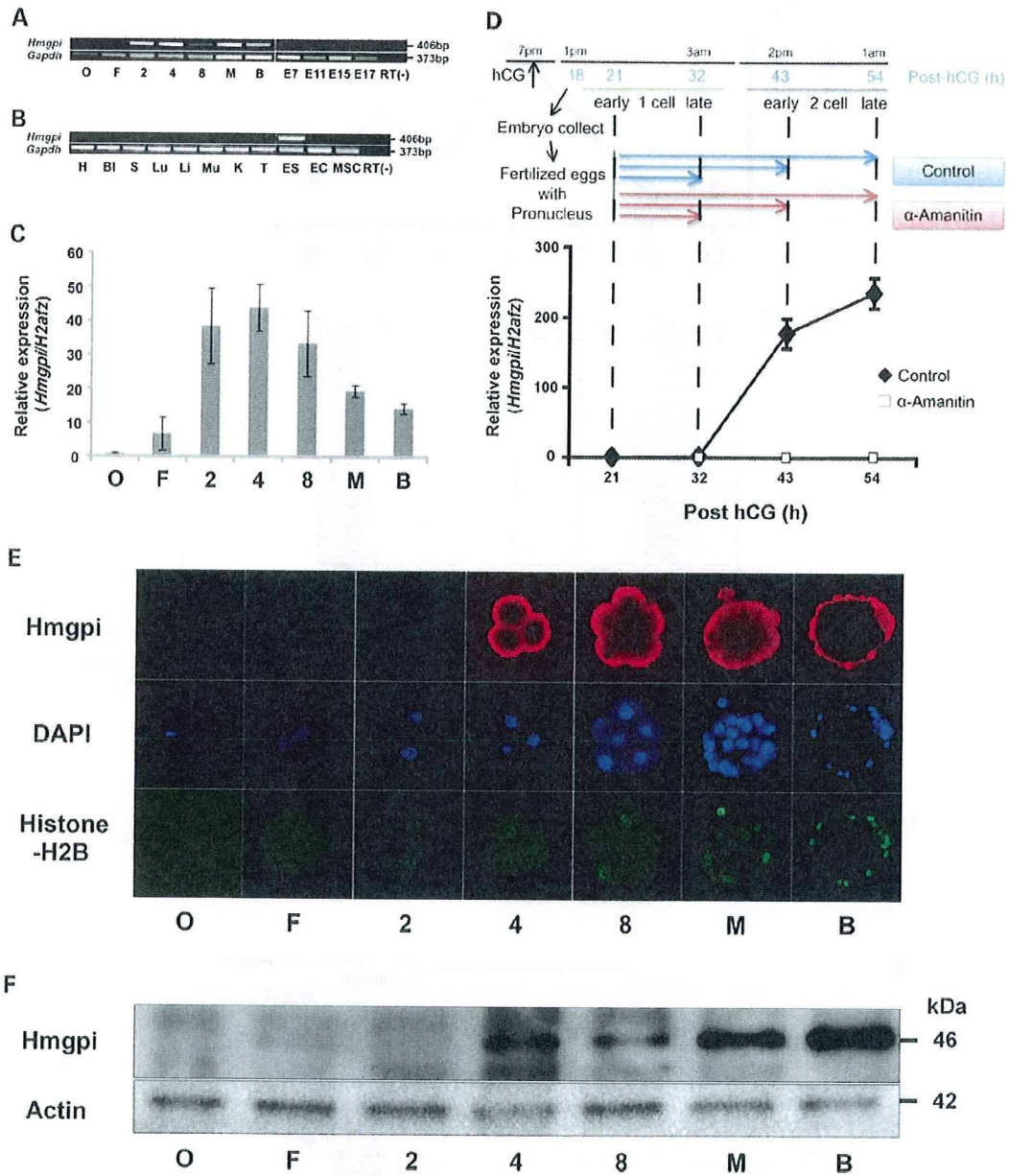
Figure 1. *In silico* analysis of *Hmgpi* expression. (**A**) Previous microarray analysis of *Hmgpi* expression. *Hmgpi* expression appeared at the 2-cell stage, peaked at the 4-cell stage and then decreased (3). (**B**) Expression sequence tag (EST) frequencies in Unigene cDNA libraries. Out of 4.7 million mouse ESTs, 16 *Hmgpi* clones were exclusively detected at the cleavage stages: 9, 2 and 5 ESTs from 2-cell, 4-cell and 8-cell libraries, respectively. (**C**) Exon–intron structures and a putative protein structure of *Hmgpi*. *Hmgpi* has three exon–intron models and one protein model. Predicted protein domains are also shown. (**D**) Conserved domains of *Hmgpi/Ubtfl1* gene in mouse, rat and human. Pairwise alignment scores of conserved domains between species were shown. (**E**) Phylogenetic tree of gene nucleotide acid sequences containing HMG domains determined by a sequence distance method and the neighbour-joining (NJ) algorithm (41) using Vector NTI software (Invitrogen, Carlsbad, CA, USA).

stage (Fig. 2A). Furthermore, significant expression of *Hmgpi* was detected in ES cells, although not in embryonic carcinoma (EC) cells nor in mesenchymal stem cells (Fig. 2B). The relative abundance of *Hmgpi* transcripts in preimplantation embryos was measured by real-time quantitative RT–PCR (qRT–PCR) analysis (Fig. 2C). Four independent experiments were conducted with four replicates of 10 embryos each. To normalize the qRT–PCR reaction efficiency, *H2afz* was used as an internal standard (20). *Hmgpi* mRNA levels increased during the 1- to 2-cell stage, peaked at the 4-cell stage, and then gradually decreased during the 8-cell to blastocyst stage (Fig. 2C). The *in silico*-predicted preimplantation-stage-specific expression pattern of *Hmgpi* was therefore validated.

Figure 2. Expression of *Hmgpi* in preimplantation embryos and other tissues. (**A**) RT–PCR analysis of *Hmgpi* expression during preimplantation and postimplantation development (E7–E17). Three sets of 10 pooled embryos were collected from each stage (O: oocyte, F: fertilized egg, 2: 2-cell embryo, 4: 4-cell embryo, 8: 8-cell embryo, M: morula, and B: blastocyst) and used for RT–PCR analysis. The predicted sizes of the PCR products of *Hmgpi* and *Gapdh* are 406 and 373 bp, respectively. No PCR products were detected in the no-RT negative control (4-cell embryo). (**B**) RT–PCR analysis of *Hmgpi* expression in adult tissues, ES cells, EC cells and mesenchymal stem cells. mRNA was isolated from mouse tissues (H: heart, Bl: bladder, S: spleen, Lu: lung, Li: liver, Mu: muscle, K: kidney, T: testis, ES: ES cells, EC: EC cells, and MSC: mesenchymal stem cells). No PCR products were detected in the no-RT negative control (ES cells). (**C**) Real-time quantitative RT–PCR analysis of *Hmgpi* expression during preimplantation development. Fold differences in amounts of *Hmgpi* mRNA from the same numbers of oocytes (O), fertilized eggs (F), 2-cell embryos (2), 4-cell embryos (4), 8-cell embryos (8), morulae (M) and blastocysts (B) are shown after normalization to an internal reference gene (mouse *H2afz*). Values are means ± SE from four separate experiments. (**D**) *De novo* (zygotic) transcription of the *Hmgpi* gene. α-Amanitin studies revealed that *Hmgpi* is transcribed zygotically, but not maternally. *Hmgpi* expression was not observed before the 2-cell stage and α-amanitin completely inhibited *de novo* transcription at the 2-cell stage (closed rhombus: control group, open square: α-amanitin-treated group). The expression levels were normalized using *H2afz* as a reference gene. Values are means ± SE from four separate experiments. (**E**) Immunocytochemical analysis of HMGPI expression. MII oocytes and preimplantation embryos were immunostained with an anti-HMGPI antibody (red) and an anti-Histone-H2B antibody as a positive control of nuclear staining (green). Nuclei are shown by DAPI staining (blue). HMGPI protein was detected from 4-cell embryos to blastocysts. (**F**) Immunoblot analysis of HMGPI during preimplantation development. An amount of extracted protein corresponding to 100 oocytes or embryos was loaded per lane. Actin was used as a loading control. The representative result is shown from three independent experiments.
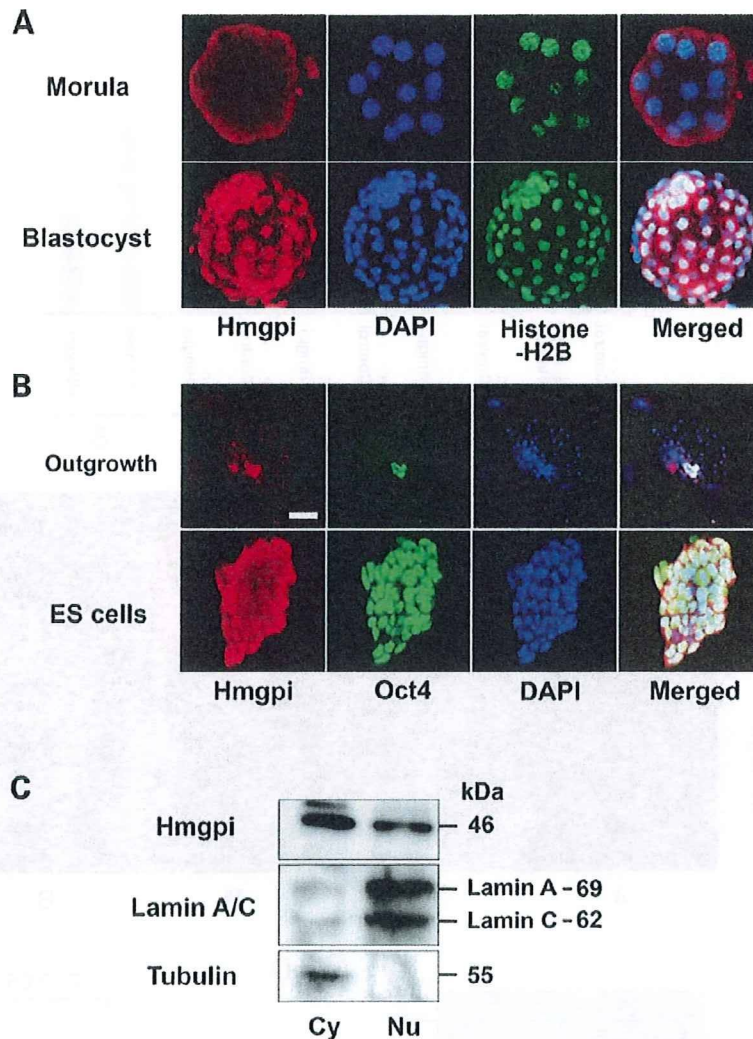
Figure 3. Localization of HMGPI in preimplantation embryos. (**A**) Nuclear translocation of HMGPI protein at the blastocyst stage. HMGPI was mainly detected in the cytoplasm of preimplantation embryos (from 4-cell embryos to morulae), but in the nuclei of blastocysts. Nuclei are shown by immunostaining with an anti-Histone-H2B antibody (green) and DAPI staining (blue). (**B**) Confocal microscopy images of blastocyst outgrowth and ES cells stained with antibodies to *Hmgpi* and *Oct4*, and with DAPI. Scale bar = 50 μM. (**C**) Western blotting analysis of HMGPI in cytoplasmic (Cy) and nuclear (Nu) fractions of ES cells. Lamin A/C and tubulin were used as markers of the nuclear and cytoplasmic fractions, respectively.

We then performed qRT–PCR analysis using α-amanitin to investigate *de novo* (zygotic) transcription of the *Hmgpi* gene. The supplementation of α-amanitin during *in vitro* culture from the 1-cell stage significantly reduced *Hmgpi* mRNA expression in the 2-cell embryos at post-hCG 43 and 53 h (early and late 2-cell stage, respectively) (Fig. 2D), implying that *Hmgpi* is transcribed zygotically during the major burst of ZGA, but not maternally.

To study the temporal and spatial expression pattern of the *Hmgpi*-encoded protein (HMGPI), we raised a polyclonal antibody against *Hmgpi* peptides. Western blot analysis of extracts from the mouse blastocysts showed only a single band corresponding to 46 kDa detected by the anti-HMGPI antibody. In addition, preincubation with the HMGPI peptide antigen abol-

ished detection of the HMGPI protein, while preincubation with a control peptide had no effect on the immunodetection (Supplementary Material, Fig. S1). Although *Hmgpi* transcription started at the 2-cell stage, peaked at the 4-cell stage and then gradually decreased until the blastocyst stage (Fig. 2C), immunostaining and immunoblotting analysis revealed HMGPI expression from the 4-cell stage until the blastocyst stage, indicating a delayed expression pattern of HMGPI compared with that of the *Hmgpi* transcript. It was also notable that both ICM cells and trophectodermal cells retained HMGPI expression in blastocysts.

On the other hand, immunostaining for HMGPI in preimplantation embryos showed a unique subcellular localization pattern. Although a putative nuclear protein due to its role
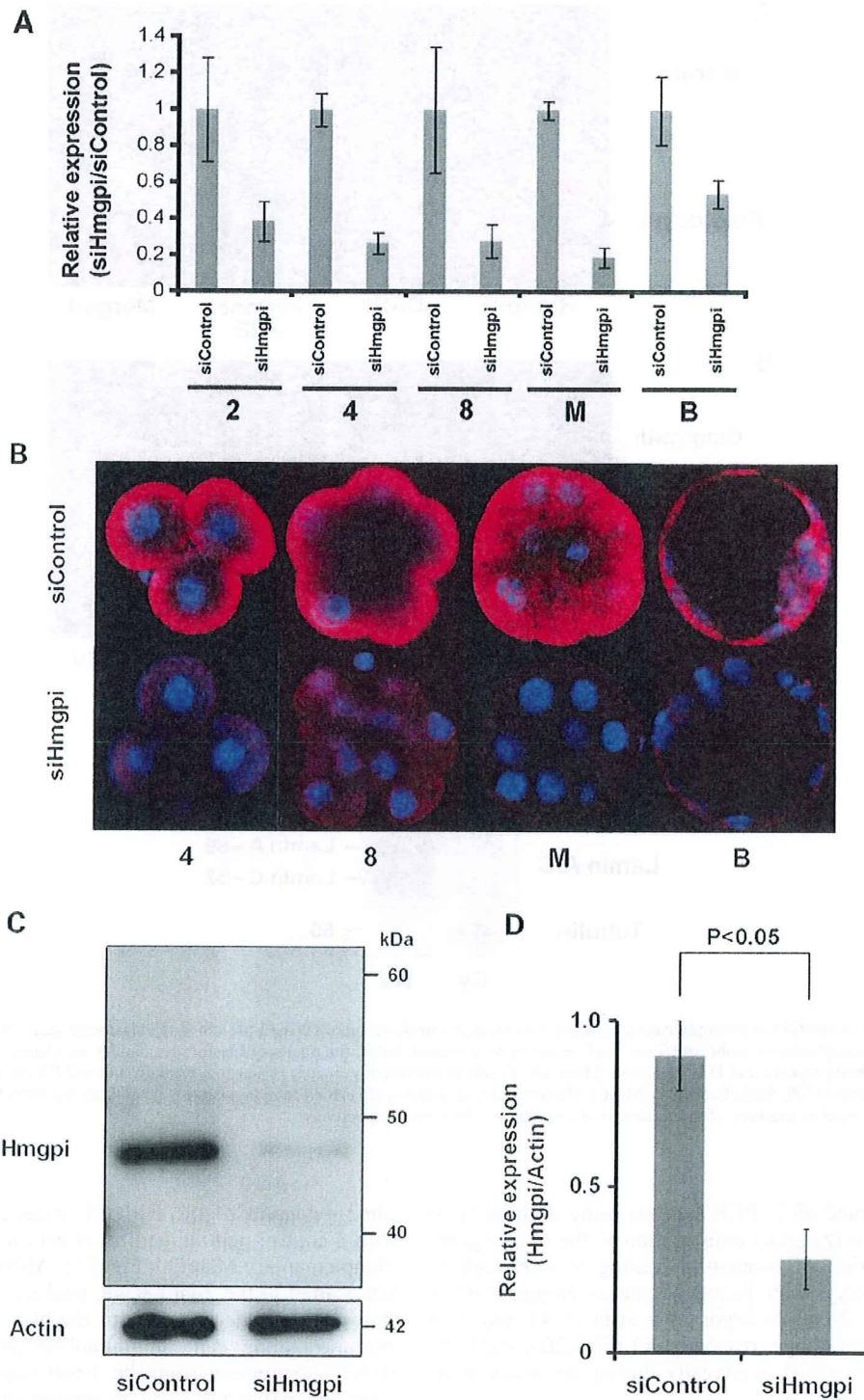
Figure 4. Loss-of-function study by siRNA technology. (**A**) Transcript levels of *Hmgpi* in embryos injected with control siRNA (siControl) and *Hmgpi* siRNA (siHmgpi) by real-time quantitative RT–PCR analysis. The expression levels were normalized using *H2afz* as a reference gene. Values are means ± SE for four separate experiments. (**B**) Laser scanning confocal microscopy images of HMGPI protein expression in a 4-cell embryo, 8-cell embryo, morula and blastocyst after injection with siControl or siHmgpi (red, HMGPI; blue, chromatin). (**C** and **D**) Immunoblot analysis of HMGPI expression at the blastocyst stage in siControl-injected and siHmgpi-injected embryos. The relative amount of HMGPI (46 kDa) was determined at the blastocyst stage (left: siControl-injected embryos, right: siHmgpi-injected embryos). The expression levels were normalized using actin expression (42 kDa) as a reference. Values are means ± SE from three separate experiments.

A

siControl

siHmgpi

B

siControl

siHmgpi

Nanog   DAPI   Oct4   DAPI

siControl

siHmgpi

Cdx2   DAPI
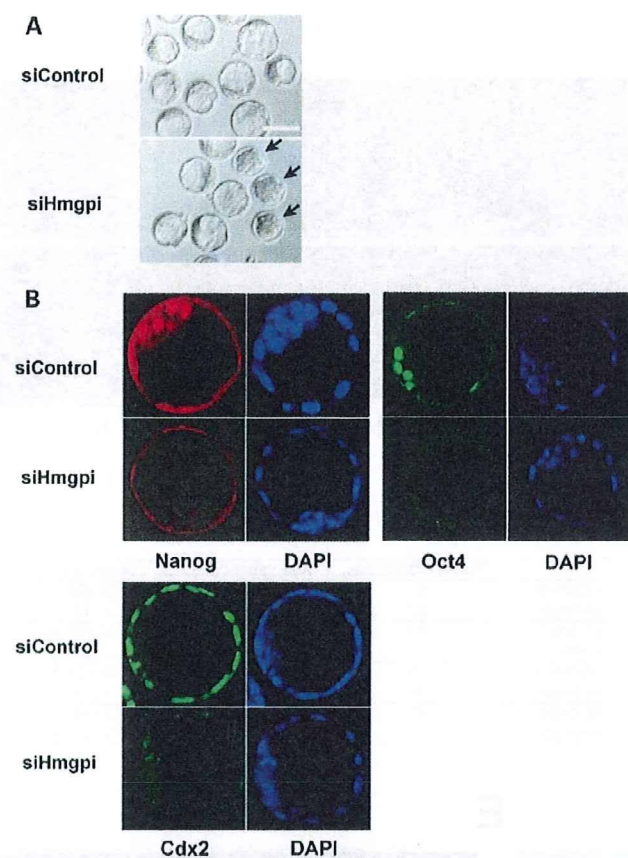
Figure 5. Function of *Hmgpi* in preimplantation development. (**A**) A pair of representative photos showing the development of embryos injected with *Hmgpi* siRNA (siHmgpi) and Control siRNA (siControl). The siHmgpi-injected embryos arrested at the morula stage are indicated by arrows. Scale bar = 100 μM. (**B**) For Nanog, Oct4 and Cdx2 immunostaining, all blastocysts in the siHmgpi-injected and siControl-injected groups were processed simultaneously. The laser power was adjusted so that the signal intensity was below saturation for the developmental stage that displayed the highest intensity and all subsequent images were scanned at that laser power. This allowed us to compare signal intensities for Nanog, Oct4 and Cdx2 expression between the siHmgpi-injected and siControl-injected embryos (Supplementary Material, Table S2).

as a transcription factor, HMGPI was detected mainly in the cytoplasm without any evidence of a nuclear localization from the 4-cell to the morula stage, suggesting a role other than transcriptional regulation (Fig. 2E). In contrast, HMGPI was localized to the nuclei rather than to the cytoplasm of blastocysts (Figs 2E and 3A). During blastocyst outgrowth, HMGPI was expressed in the nuclear region of most outgrowing cells, with scant amounts detected in the cytoplasm (Fig. 3B). Interestingly, Oct4-positive cells derived from the ICM showed particularly strong positive staining for HMGPI in the nucleus, suggesting a specific role as a nuclear protein in ES cells (Fig. 3B). On more closely examining HMGPI in ES cells, we found that almost all the Oct4-positive undifferentiated ES cells in a colony also expressed HMGPI (Fig. 3B), and immunoblotting confirmed HMGPI expression in both nuclear and cytoplasmic fractions of ES cells (Fig. 3C).

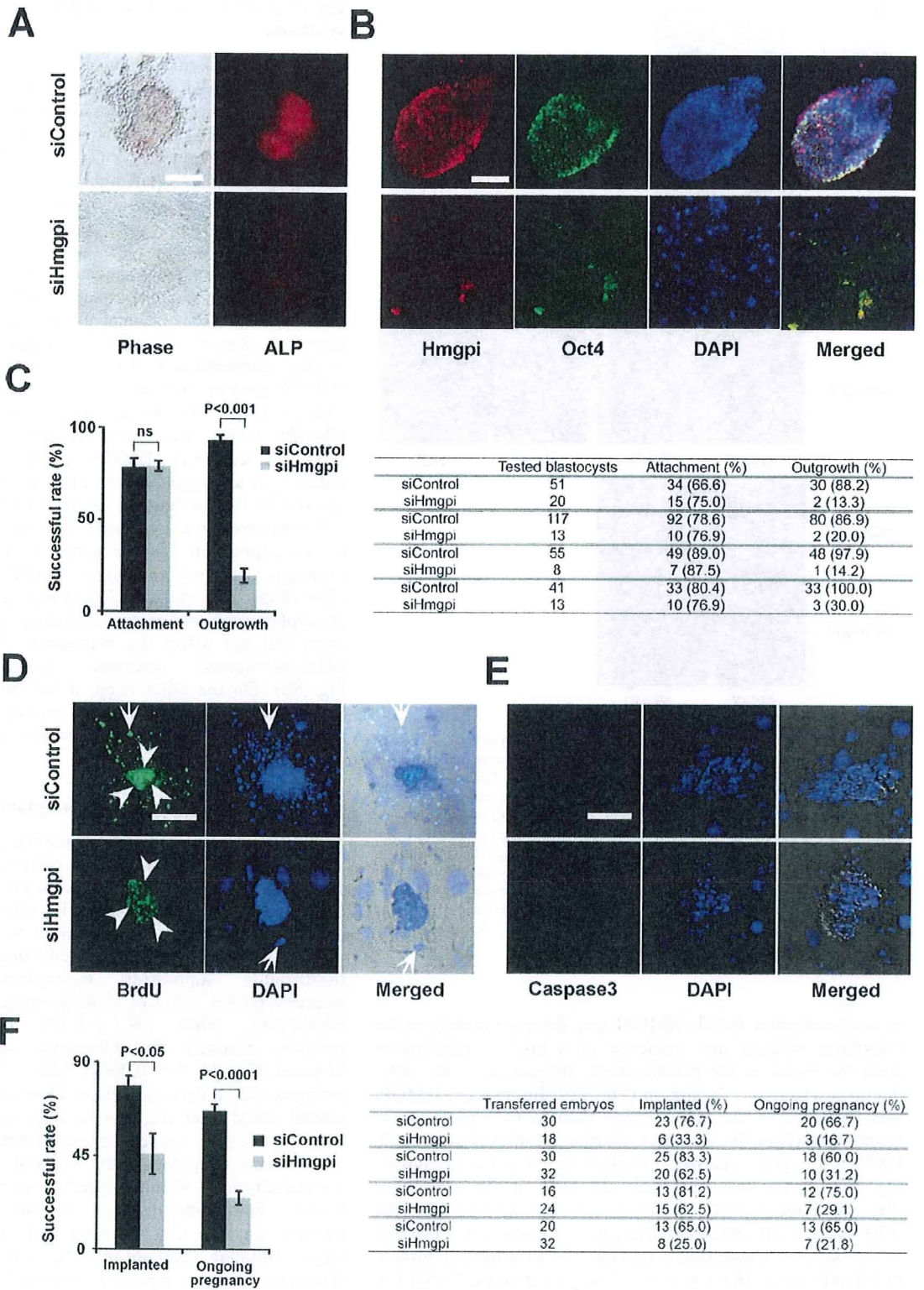## Effect of siRNA on *Hmgpi* mRNA level and protein synthesis

To investigate a role of *Hmgpi* in early embryonic development, we knocked down *Hmgpi* expression in mouse preimplantation embryos. We employed an oligonucleotide-based siRNA (denoted here siHmgpi and obtained from PE Applied Biosystems, Foster City, CA, USA). Zygotes injected with *Hmgpi* siRNAs (siHmgpi) or control siRNA (siControl) and non-injected zygotes as negative controls were cultured. *Hmgpi* expression was severely suppressed in the siHmgpi-injected embryos, and significantly lower than those in the siControl-injected or non-injected embryos (Fig. 4A). The siControl-injected embryos did not show any difference from the non-injected embryos in *Hmgpi* expression (data not shown). In addition, immunofluorescent staining clearly demonstrated that the siRNA injection reduced HMGPI protein expression in an individual preimplantation embryo (Fig. 4B). In the same set of experiments, the HMGPI levels were also assayed by western blotting (Figs 4C and 4D). HMGPI expression was significantly reduced in siHmgpi-injected blastocysts (0.89 ± 0.10) compared with that in negative controls (0.28 ± 0.08; $P < 0.05$).

Furthermore, we confirmed that siHmgpi had no influence on the expression of other genes with sequence similarities to *Hmgpi*, namely *Ubtf, Hmgb1, Hmgb2* and *Hmgb3*. Although *Ubtf, Hmgb1, Hmgb2* and *Hmgb3* were all expressed in control preimplantation embryos, the siHmgpi construct used in this study did not affect the expression of these genes in the siHmgpi-injected embryos (Supplementary Material, Fig. S2). On the other hand, it has been demonstrated that loss-of-function of these genes produces no distinct phenotypes at the pre- and peri-implantation stages (21).

Effect of *Hmgpi* siRNA on preimplantation development

To study the function of *Hmgpi* during preimplantation development, siHmgpi-injected or siControl-injected zygotes were cultured *in vitro* until the blastocyst stage. The embryos injected with siHmgpi at 21–23 h after hCG administration often failed to become blastocysts at 3.5 days postcoitum (dpc) (Fig. 5A). In addition, the reduction in Hmgpi expression significantly suppressed preimplantation development, whereby $68.9 \pm 1.3\%$ of siHmgpi-injected embryos became blastocysts, while $94.1 \pm 1.3\%$ of siControl-injected embryos reached the blastocyst stage (Supplementary Material, Fig. S3; $P < 0.0001$). Most of the siHmgpi-injected embryos that failed to become blastocysts showed developmental arrest after the morula stage and did not appear to form blastocoels, suggesting impairment of trophectodermal development (Supplementary Material, Fig. S3). To analyze the phenotype of siHmgpi-injected embryos further, we performed immunofluorescence staining of lineage-specific markers such as Cdx2, Nanog and Oct4 at the blastocyst stage. Although siHmgpi-injected embryos that reached the blastocyst stage appeared morphologically intact, the expression of lineage-specific markers was reduced (Fig. 5B). Cdx2, which is required for implantation and extra-embryonic development, was particularly and markedly down-regulated in trophectodermal cells, while Nanog and Oct4

A

siControl / siHmgpi

Phase   ALP

B

siControl / siHmgpi

Hmgpi   Oct4   DAPI   Merged

C

P<0.001

ns

Successful rate (%)

■ siControl
■ siHmgpi

Attachment   Outgrowth

	Tested blastocysts	Attachment (%)	Outgrowth (%)
siControl	51	34 (66.6)	30 (88.2)
siHmgpi	20	15 (75.0)	2 (13.3)
siControl	117	92 (78.6)	80 (86.9)
siHmgpi	13	10 (76.9)	2 (20.0)
siControl	55	49 (89.0)	48 (97.9)
siHmgpi	8	7 (87.5)	1 (14.2)
siControl	41	33 (80.4)	33 (100.0)
siHmgpi	13	10 (76.9)	3 (30.0)

D

siControl / siHmgpi

BrdU   DAPI   Merged

E

Caspase3   DAPI   Merged

F

P<0.05   P<0.0001

Successful rate (%)

■ siControl
■ siHmgpi

Implanted   Ongoing pregnancy

	Transferred embryos	Implanted (%)	Ongoing pregnancy (%)
siControl	30	23 (76.7)	20 (66.7)
siHmgpi	18	6 (33.3)	3 (16.7)
siControl	30	25 (83.3)	18 (60.0)
siHmgpi	32	20 (62.5)	10 (31.2)
siControl	16	13 (81.2)	12 (75.0)
siHmgpi	24	15 (62.5)	7 (29.1)
siControl	20	13 (65.0)	13 (65.0)
siHmgpi	32	8 (25.0)	7 (21.8)

were likewise downregulated in ICM cells of the siHmgpi-injected embryos (Fig. 5B and Supplementary Material, Table S2). Thus, *Hmgpi* is essential for the earliest embryonic development; both ICM and trophectodermal development.

Effect of *Hmgpi* siRNA on *in vivo* and *in vitro* peri-implantation development

To investigate the role of *Hmgpi* in proliferation of the ICM and trophectodermal cells, siHmgpi-injected and siControl-injected embryos were further cultured *in vitro* from the blastocyst stage, and attachment and outgrowth of each embryo on gelatin-coated culture plates was examined. HMGPI expression in siHmgpi-injected embryos was significantly reduced, and immunostaining showed that many colonies of ICM cells in the embryos collapsed during outgrowth culture (Fig. 6A and B). Although the vast majority of ICMs from siControl-injected embryos showed successful attachment (80.3 ± 4.9%) and vigorous outgrowth (96.2 ± 2.7%), those from siHmgpi-injected embryos failed to proliferate or produced only a residual mass (19.3 ± 3.8%) despite successfully attaching (79.0 ± 2.8%) (Fig. 6C; attachment ns; outgrowth, *P* < 0.001). These results implied that *Hmgpi* is essential for proliferation of ICM and trophectodermal cells in peri-implantation development, and for derivation of ES cells.

We then investigated cell proliferation and apoptosis during blastocyst outgrowth. Comparable incorporation of BrdU in blastocyst outgrowths of siHmgpi-injected embryos was less than that of siControl-injected embryos. Proliferation was significantly reduced in ICM-derived cells and dramatically suppressed in trophoblast cells (Fig. 6D). Embryonic fibroblasts were used as a feeder layer in this study and could support ICM cells, thus proliferation should have proceeded regardless of trophectodermal cell support. Therefore, the collapsed ICM-derived colonies in the current experiment were not a secondary effect of reduced proliferation in trophoblast cells, but a direct effect of the siHmgpi-induced decrease in ICM proliferation. Apoptosis was not detected in any cells during blastocyst outgrowth of siHmgpi-injected embryos, based on the absence of active caspase3 (Fig. 6E). Taken together, these findings show that *Hmgpi* is indispensable for proliferation of the ICM and trophectodermal cells in peri-implantation development and for the generation of ES cells.

Finally, we tested whether the experimental blastocysts could develop *in vivo* by transferring siHmgpi-injected and siControl-injected blastocysts into the uterus of pseudopregnant mice. Only 45.8 ± 9.7 and 24.7 ± 3.3% of blastocysts injected with siHmgpi implanted and developed, respectively, whereas most of the siControl-injected embryos showed successful implantation and ongoing development (76.5 ± 4.0 and 66.6 ± 3.3%, respectively) (Fig. 6F; implanted, *P* < 0.05; ongoing pregnancy, *P* < 0.0001). These results confirmed a role for *Hmgpi* in peri-implantation embryonic development.

DISCUSSION

We previously analyzed the dynamics of global gene expression changes during mouse preimplantation development (3). Understanding these preimplantation stages is important for both reproductive and stem cell biology. Many genes showing wave-like activation patterns (e.g. ZGA and MGA) during preimplantation were identified, and any or all of these may contribute to the complex gene regulatory networks. *Hmgpi*, one of the few novel preimplantation-specific genes, is involved in early development, implantation and ES cell derivation.

Structure-based prediction of *Hmgpi* function

Structural information about a protein sometimes hints at functional mechanisms, which remain unknown for *Hmgpi*'s clear role in early embryonic development. The HMG family proteins are abundant nuclear proteins that bind to DNA in a non-sequence-specific manner, influence chromatin structure and enhance the accessibility of binding sites to regulatory factors (17). Based on the number and the type of HMG domains, *Hmgpi* is relevant to the HMGB subfamily, characterized by containing two HMG-box domains ('HMG-box' or 'HMG-UBF_HMG-box'), rather than either the HMGA or HMGN subgroups. *Hmgpi* is also known as *Ubtfl1* in the NCBI gene database, based on sequence similarity to *Ubtf*, a well-known ZGA gene (3,22). *Ubtf*, encoding a SANT domain and six HMG-box domains, functions exclusively in RNA polymerase I (Pol I) transcription (23) and acts through its multiple HMG boxes to induce looping of DNA, which creates a nucleosome-like structure to modulate tran-

Figure 6. Function of *Hmgpi* in peri-implantation development. (A) Blastocyst outgrowth and alkaline phosphatase (AP) activity in the siHmgpi-injected and siControl-injected embryos, carried out according to a standard procedure (42). Representative images of phase-contrast microscopy for blastocyst outgrowth and fluorescent immunocytochemistry for AP are shown. Scale bar = 100 μM. (B) Confocal microscopy images of blastocyst outgrowth for the siHmgpi-injected and siControl-injected embryos, stained with antibodies to Hmgpi and Oct4. Nuclei are shown by DAPI staining. Scale bar = 100 μM. (C) Successful rate of blastocyst outgrowth for siHmgpi-injected and siControl-injected embryos. Successful outgrowth in this assay was indicated by the presence of proliferating cells after 6 days in culture. The experiment was repeated four times. (D) BrdU incorporation assay for blastocyst outgrowth of the siHmgpi-injected and siControl-injected embryos. Cell proliferation was determined by BrdU incorporation (ICM: arrowhead, trophectodermal cells: arrow). The trophectodermal component contained few cells and BrdU incorporation was confined to the ICM core; however, cell proliferation was reduced in the blastocyst outgrowth of siHmgpi-injected embryos compared with that of the siControl-injected embryos. Nuclei are shown by DAPI staining. Scale bar = 100 μM. (E) Immunocytochemistry with an anti-caspase3 antibody in blastocyst outgrowth of the siHmgpi-injected and siControl-injected embryos. Apoptotic cells were not apparent in the blastocyst outgrowth of either injected embryo. Nuclei are shown by DAPI staining. Scale bar = 100 μM. (F) Successful rate of siHmgpi-injected and siControl-injected embryo transfer. We transferred 3.5 dpc blastocysts into the uteri of 2.5 dpc pseudopregnant ICR female mice. The pregnant ICR mice were sacrificed on day 12.5 of gestation and the total numbers of implantation sites and of live and dead embryos/fetuses were counted. The experiment was repeated four times.

scription of the 45S precursor of ribosomal RNA (rRNA) by Pol I (24,25). Because the association of UBTF with rRNA genes *in vivo* is not restricted to the promoter and extends across the entire transcribed portion, UBTF promotes the formation of nucleolar organizer regions, indicative of 'open' chromatin (26). Based on the sequence similarity between UBTF and HMGPI, HMGPI might also bind to DNA in a non-specific manner, and modulate chromatin during peri-implantation when dynamic chromatin change is essential.

Alternatively, HMGPI may act as a cytokine during preim-plantation development in a similar manner to HMGB1. HMGB proteins are found primarily in the cell nucleus, but also to varying extents in the cytosol (27,28), and have been suggested to shuttle between compartments (17). HMGB1 is indeed passively released from nuclei upon cell death and actively secreted as a cytokine (29), and the addition of recom-binant HMGB1 into culture medium enhances *in vitro* devel-opment of mouse zygotes to the blastocyst stage in the absence of BSA supplementation (30). Although HMGPI failed to be detected in culture media after *in vitro* culture of preimplantation embryos or ES cells in this study (data not shown), two different modes of Hmgpi action, chromatin modulator and secreted mediator, should be taken into con-sideration as discussed later.

Role of *Hmgpi* during peri-implantation

The HMGPI protein was first detected in 4-cell embryos and then abundantly expressed in 8-cell embryos, morulae, ICM, trophectoderm and ES cells. Although *Hmgpi* transcription peaked at the 4-cell stage, the most dramatic siRNA effect appeared at the blastocyst and subsequent stages. This discre-pancy between temporal expression and phenotype is attribu-ted to three possible mechanisms. First, protein expression is generally delayed from transcription, indicated here by the *Hmgpi* transcripts and HMGPI protein expression peaking at the 4-cell stage and blastocyst stage, respectively. Similarly, *Stella* (31) and *Pms2* (32) are maternal-effect genes, but do not cause developmental loss until later preimplantation stages. A second possibility is the incompleteness of siRNA knockdown. One limitation of such knockdown experiments is the potential variability in levels of silencing of a target gene, which could in turn underlie the observed phenotypic variability in the present study. Embryos with complete sup-pression of Hmgpi may exhibit developmental arrest at earlier stages (e.g. at the morula stage), while those with less suppression may not display a phenotype until the later stages (e.g. at the implantation stage). Ideally, the suppression level of each embryo could be experimentally analyzed to cor-relate with the phenotype. The third possibility is spatial trans-location of HMGPI protein in the blastocyst cells. The HMGPI expression pattern indicated differential spatial requirements during early embryogenesis, supported by the apparent ability of HMGPI to shuttle between the nucleus and the cyto-plasm; the cytoplasmic HMGPI observed from the 4-cell to morula stages and the nuclear HMGPI in blastocysts and ES cells could have different functions. A bipartite nuclear local-ization signal (NLS) peptide (FKKEKEDFQKKMRQFKK) similar to NLS of HMGN2/HMG-17 (33) is also present in the HMGPI sequence. Thus, the nuclear HMGPI in blastocysts

and ES cells might exert a critical transcriptional role to regu-late gene expression essential for peri-implantation develop-ment. Indeed, the siHmgpi-induced knockdown of *Hmgpi* expression downregulated *Cdx2* in trophectodermal cells and *Oct4* and *Nanog* in ICM cells, with subsequently reduced pro-liferation of trophectodermal cells and ICM-derived cells during blastocyst outgrowth.

Genes indispensable for derivation of ES cells

Like *Hmgpi*, *Zscan4* is another exclusively zygotic gene not expressed at any other developmental stage (13). *Zscan4* is a putative transcription factor harboring a SCAN domain and zinc finger domains, and transcribed not only in preimplanta-tion embryos but also in ES cells (13). Reduction of *Zscan4* by RNA interference showed a phenotype similar to that induced by *Hmgpi* knockdown: developmental deterioration at the pre-implantation stages, especially cleavage pause at 2-cell stage, and failure in blastocyst outgrowth, ES-cell derivation and implantation. Thus, a preimplantation-specific gene expression pattern could indicate a function in ES-cell derivation and/or maintenance. Indeed, *Hmgpi* was also expressed in entire ES colonies, whereas *Zscan4* shows a peculiar mosaic expression pattern in undifferentiated ES cell colonies. Furthermore, the *Hmgpi* gene is highly expressed in ES cells, but not in EC cells; *Hmgpi* is thus eligible as a putative ECAT (ES cell-associated transcript), whose ESTs are overrepresented in cDNA libraries from ES cells compared with those from somatic tissues and other cell lines including EC cells (34). It is also likely that *Hmgpi* is expressed in iPS cells, based on *in silico* analyses of expression profiles [NCBI GEO data-base, e.g. GSE10806 (35)]. Thus, *Hmgpi* is likely to have a role in maintaining pluripotent cells, since the ECATs such as *Nanog*, *Eras* and *Gdf3* are required for pluripotency and proliferation of ES cells (34,36,37). In the current study, *Hmgpi* was indeed involved in blastocyst outgrowth of ICM cells. On the other hand, several genes including ECAT members have been implicated in trophectodermal develop-ment as well as in early embryonic development. Like *Hmgpi* that was expressed in both ICM cells and trophectoder-mal cells, *Dnmt3l/Ecat7* has a role in embryonic and extra-embryonic tissues in early developmental stages. *DNMT3L* is recruited by *DNMT3A2* to chromatin (38) to function in DNA methylation in ES cells, and defects in maternal *DNMT3L* induce a differentiation defect in the extra-embryonic tissue (39). The reduced CDX2 expression in blastocysts and poor BrdU incorporation during blastocyst out-growth following siHmgpi knockdown suggested the potential involvement of *Hmgpi* in trophectodermal development.

In summary, *Hmgpi* is required early on in mammalian development to generate healthy blastocysts that implant successfully and produce ES cells. HMGPI translocates into the nucleus from cytoplasm at the blastocyst stage, which is importantly a turning point of early embryonic development when DNA-methylation levels are at their lowest and implan-tation takes place. The nuclear HMGPI in blastocysts and ES cells is expected to act as a transcription factor to regulate gene expression networks underlying the generation, self-renewal and maintenance of pluripotent cells. Because E7 embryos have already stopped expressing *Hmgpi*, it is likely

that *Hmgpi* stage-specifically regulates a set of genes that drive peri-implantation development. It will be valuable to identify both cofactors that bind HMGPI and recognize specific DNA sequences, as well as genes that are regulated by *Hmgpi* using ES cells. A better understanding of the *Hmgpi* transcriptional network will also improve culture methods for healthy blastocysts and for generating, maintaining and differentiating ES cells.

MATERIALS AND METHODS

Identification of the mouse *Hmgpi* gene by *in silico* analysis

Preimplantation-specific genes were identified based on global gene expression profiling of oocytes and preimplantation embryos (3,40) and expressed sequence tag (EST) frequencies in the Unigene database. SMART (19) was used for domain prediction analysis. Orthologous relationships between HMG family genes were identified from phylogenetic-tree amino acid sequences determined by a sequence distance method and the Neighbor Joining (NJ) algorithm (41) using Vector NTI software (Invitrogen, Carlsbad, CA, USA).

Collection and manipulation of embryos

Six- to 8-week-old B6D2F1 mice were superovulated by injecting 5 IU of pregnant-mare serum gonadotropin (PMS; Calbiochem, La Jolla, CA, USA) followed by 5 IU of human chorionic gonadotropin (HCG; Calbiochem) 48 h later. The Institutional Review Board of the National Research Institute for Child Health and Development, Japan granted ethics approval for embryo collection from the mice. Unfertilized eggs were harvested 18 h after the HCG injection by a standard published method (42), and the cumulus cells were removed by incubation in M2 medium (EmbryoMax M-2 Powdered Mouse Embryo Culture Medium; Millipore, Billerica, MA, USA) supplemented with 300 μg/ml hyaluronidase (Sigma-Aldrich, St Louis, MO, USA). The eggs were then thoroughly washed, selected for good morphology and collected. Fertilized eggs were also harvested from mated superovulated mice in the same way as unfertilized eggs and embryos with two pronuclei (PN) were collected to synchronize *in vitro* embryo development. Fertilized eggs were cultured in synthetic oviductal medium enriched with potassium (EmbryoMax KSOM Powdered Mouse Embryo Culture Medium; Millipore) at 37°C in an atmosphere of 95% air/5% CO_2. Cultured blastocysts were transferred into pseudopregnant recipients as described previously (42). We transferred 3.5 dpc blastocysts into the uteri of 2.5 dpc pseudopregnant ICR female mice. RNA interference experiments were carried out by microinjecting <10 pl (25 ng/μl) of oligonucleotides (siHmgpi and siControl) into the cytoplasm of zygotes. The optimal siRNAs were determined by testing different concentrations (5, 10, 25 and 50 ng/μl) of three siRNAs (PE Applied Biosystems, Foster City, CA, USA), resuspended and diluted with the microinjection buffer (Millipore). Their target sequences are listed in Supplementary Material, Table S3. More than 10 independent experiments were performed to study the effect of *Hmgpi* knockdown on preimplantation development and implantation.

Culture of ES cells and blastocyst outgrowth

A mouse ES cell line (B6/129ter/sv line) was first cultured for two passages on gelatin-coated culture dishes in the presence of leukemia inhibitory factor (LIF) to remove contaminating feeder cells. Cells were then seeded on gelatin-coated 6-well plates at a density of $1-2 \times 10^5$/well ($1-2 \times 10^4$/cm^2) and cultured for 3 days in complete ES medium: KnockOut DMEM (Invitrogen) containing 15% KnockOut Serum Replacement (KSR; Invitrogen), 2000 U/ml ESGRO (mLIF; Chemicon, Temecula, CA, USA), 0.1 mM non-essential amino acids, 2 mM GlutaMax (Invitrogen), 0.1 mM beta-mercaptoethanol (2-ME; Invitrogen) and penicillin/streptomycin (50 U/50 μg/ml; Invitrogen). Blastocyst outgrowth experiments were carried out according to a standard procedure (42). In brief, zona pellucidae of blastocysts at 3.5 dpc were removed using acidic Tyrode's solution (Sigma). The blastocysts were cultured individually in the ES medium on gelatinized chamber slides at 37°C in an atmosphere of 5% CO_2. The cultured cells were examined and photographed daily. Alkaline phosphatase activity was measured using a specific detection kit (Vector Laboratories, CA, USA) after 6 days in culture. Four independent experiments were performed.

Immunostaining of oocytes and preimplantation embryos

Samples were fixed in 4% paraformaldehyde (Wako Pure Chemical, Osaka, Japan) with 0.1% glutaraldehyde (Wako) in phosphate-buffered saline (PBS) for 10 min at room temperature (RT), and then permeabilized with 0.5% Triton X-100 (Sigma) in PBS for 30 min. Immunocytochemical staining was performed by incubating the fixed samples with primary antibodies for 60 min, followed by secondary antibodies for 60 min. A polyclonal antibody to mouse HMGPI was raised in rabbits against three synthesized peptides designed according to sequence specificity, homology between mouse and human HMGPI, antigenicity, hydrophilicity and synthetic suitability [(i) CIQGHHDGAQSSRQDFTD, (ii) CMSMSGG RSSKFGRTEQS, (iii) ESPRTVSSDMKFQGC; Medical & Biological Laboratories Co, Nagoya, Japan). The anti-HMPGI was used at 1:300 dilution, followed by Alexa Fluor 546 goat anti-rabbit IgG (Molecular Probes, Invitrogen) as the secondary antibody. The anti-Histone H2B antibody (Medical & Biological Laboratories Co, Nagoya, Japan) was used at 1:300 dilution as positive control of nuclear staining, followed by Alexa Fluor 488 goat anti-mouse IgG (Molecular Probes, Invitrogen) as the secondary antibody. Blastocysts were immunostained using a monoclonal anti-Oct4 antibody (mouse IgG2b isotype, 200 μg/ml; Santa Cruz Biotechnology, Santa Cruz, CA, USA), rabbit polyclonal anti-Nanog antibody (ReproCELL, Tokyo, Japan), mouse monoclonal anti-Cdx2 antibody (CELL MARQUE, Rocklin, CA, USA), mouse monoclonal anti-BrdU antibody (Santa Cruz) and rabbit monoclonal anti-active caspase 3 (Abcam) antibody, all diluted at 1:50–300. The appropriate secondary antibodies (IgG) were diluted at 1:300 and supplied by Molecular Probes/Invitrogen: goat anti-rabbit IgG conjugated with Alexa Fluor 546 and goat anti-mouse IgG(H + L) conjugated with Alexa Fluor 488. The cellular DNA (nuclei) was stained with 4′,6-diamidino-2-phenylindole (DAPI; Wako; diluted

1:300). The cells were then washed with PBS and viewed by laser confocal microscopy (LSM510, Zeiss). For HMGPI immunostaining, all samples were processed simultaneously. The laser power was adjusted so that the signal intensity was below saturation for the developmental stage that displayed the highest intensity and all subsequent images were scanned at that laser power. This allowed us to compare signal intensities for HMGPI expression at different developmental stages. The other molecules in blastocysts and outgrowth were viewed and imaged as for the HMGPI expression.

Immunocytochemistry of blastocyst outgrowths and ES cells

Cultured ES cells and blastocyst outgrowths were fixed with 4% paraformaldehyde for 10 min at 4°C, treated with 0.1% Triton X-100 (Sigma) in PBS for 15 min at RT, and then incubated for 30 min at RT in protein-blocking solution consisting of PBS supplemented with 5% normal goat serum (Dako, Glostrup, Denmark). The samples were then incubated overnight with the primary antibodies to OCT4, HMGPI, BrdU or active caspase 3 in PBS at 4°C. The cells were then extensively washed in PBS and incubated at RT with Alexa Fluor 488 goat anti-mouse IgG1 (anti-OCT4 and anti-BrdU antibodies, diluted 1:300; Molecular Probes) or Alexa Fluor 546 goat anti-rabbit IgG(H + L) (anti-HMGPI and anti-caspase 3 antibodies, diluted 1:300), and nuclei were counterstained with DAPI for 30 min. To prevent fading, cells were then mounted in Dako fluorescent mounting medium (Dako).

Incorporation of bromodeoxyuridine (BrdU)

E3.5 blastocysts and blastocyst outgrowths were cultured for 16 h in KSOM and ES medium, respectively, supplemented with 10 μM BrdU (Sigma). Samples were then fixed in 4% paraformaldehyde for 20 min, washed in PBS and then treated with 0.5 M HCl for 30 min.

RNA extraction and real-time quantitative reverse transcriptase (qRT)–PCR

Embryos for qRT–PCR analysis were collected at 18 h post-hCG and cultured as described above. They were harvested at 0.5, 1.25, 1.75, 2.25, 2.75 and 3.75 dpc to obtain fertilized eggs 2-cell, 4-cell, 8-cell, morula and blastocyst embryos, respectively. Three subsets of 10 and 50 synchronized and intact embryos were transferred in PBS supplemented with 3 mg/ml polyvinylpyrrolidone (PVP) and stored in liquid nitrogen. Total RNA from 10 and 50 embryos was extracted using the PicoPure RNA Isolation Kit (Arcturus, La Jolla, CA, USA). The reverse transcription reaction, primed with polyA primer, was performed using Superscript III reverse transcriptase (Invitrogen) following the manufacturer's instructions. Total RNA isolated was reverse transcribed in a 20 μl volume. The resulting cDNA was quantified by qRT–PCR analysis using the SYBR Green Realtime PCR Master Mix (Toyobo, Osaka, Japan) and ABI Prism 7700 Sequence Detection System (PE Applied Biosystems) as described previously (43). An amount of cDNA equivalent to 1/2 an embryo was used for

each real-time PCR reaction with a minimum of three replicates, with no-RT and no-template controls for each gene. Data were normalized against *H2afz* by the ΔΔCt method (44). PCR primers for the genes of *Hmgpi*, *H2afz* and *Gapdh* were listed in Supplementary Material, Table S4. Calculations were automatically performed by ABI software (Applied BioSystems). For alpha-amanitin studies, fertilized eggs were first harvested at 18 h post-hCG, instead of eggs already advanced to the two-pronucleus stage. After 3 h of incubation, eggs that carried both male and female pronuclei were selected at 21 h post-hCG and randomly assigned to two experimental groups: with and without addition of alpha-amanitin to the culture medium. The eggs were further cultured in KSOM at 37°C in an atmosphere of 5% CO_2 until the specified time point (32, 43 and 54 h post-hCG). Embryos used for alpha-amanitin studies and RNA interference experiments were subjected to qRT–PCR as described for the normal preimplantation embryos.

Immunoblot analysis

Protein samples from embryos were solubilized in Sample Buffer Solution without 2-ME (Nacalai Tesque, Kyoto, Japan), resolved by NuPAGE Novex on Tris-acetate mini gels (Invitrogen), and transferred to Immobilon-P transfer membrane (Millipore). The membrane was soaked in protein blocking solution (Blocking One solution, Nacalai) for 30 min at RT before an overnight incubation at 4°C with primary antibody, also diluted in blocking solution. The membrane was then washed three times with TBST (Tris-buffered saline with 0.1% Tween-20), incubated with a horseradish peroxidase-conjugated secondary antibody (0.04 μg/ml) directed against the primary antibody for 60 min, and washed three times with TBST. The signal was detected by enhanced chemiluminescence (SuperSignal West Dura Extended Duration Substrate, Thermoscientific, Rockford, IL, USA) following the manufacturer's recommendations. The intensity of the band was quantified using NIH Image J software. Briefly, the signal was outlined and the mean intensity and background fluorescence were measured. The specific signal was calculated by dividing the band intensities for HMGPI by those for actin.

Statistical analysis

Differences between groups were evaluated statistically using Student's *t*-test or ANOVA, with *P*-values < 0.05 considered significant.

SUPPLEMENTARY MATERIAL

Supplementary Material is available at *HMG* online.

ACKNOWLEDGEMENTS